Molecular Dynamics Simulation of O_3 Photolysis by Ultraviolet Light in Solid Argon

XI-JING NING, QI-ZONG QIN

Laser Chemistry Institute, Fudan University, Shanghai 200433, China

Received 24 July 1998; accepted 23 November 1998

ABSTRACT: A technique of time reversal is used to simulate the trapping-site structure of O_3 isolated in an argon matrix. It is found that the most probable trapping site is single substitutional. The UV photodissociation of O_3 in Ar matrices is simulated by molecular dynamics. It is shown that the photolysis channels of O_3 in the single trapping site are seriously hindered by the matrix cage. The photolysis quantum yield obtained via our simulations is in agreement with corresponding measurements. © 1999 John Wiley & Sons, Inc. J Comput Chem 20: 623–628, 1999

Keywords: molecular dynamics; matrix isolation; ozone; photolysis

Introduction

Due to the importance of O_3 in photochemistry of the earth's atmosphere, a great deal of effort has been devoted to investigation of the photodissociation dynamics of ozone in the gas phase[1] or trapped in cryogenic matrices.[2,3] Photolysis of O_3 in the Hartley band (220–310 nm) leads to fragmentation via[4]:

$$O_3(X^1A_1) + h\nu \rightarrow \begin{cases} O_2(^1\Delta_g) + O(^1D) & (1) \\ O_2(^3\Sigma_g^-) + O(^3P) & (2) \end{cases}$$

Correspondence to: X.-J. Ning; e-mail: quqin@srcap.stc.sh.cn

The quantum yield for photodissociation of the free ozone molecule was found to be close to unity.[5] An experimental measurement[2] showed that the quantum yield for photodissociation of O_3 diluted in solid argon is one or two orders of magnitude smaller than that of free ozone. It is even more noteworthy that the cage escape probability is dramatically dependent on the matrix temperature, even though the excess translational energy of the photogenerated O atoms is about two orders of magnitude greater than the thermal energies of the matrix.[2]

Obviously, the trapping-site structures (the matrix structures around the ozone molecules) should be responsible for the photolysis characteristics of O_3 isolated in Ar matrices. To the best of our knowledge, no theoretical study has been under-

CCC 0192-8651 / 99 / 060623-06

taken to investigate the dynamics of O_3 photolysis in cryogenic matrices. In this article, the trapping-site structures around O_3 are determined in the next section by a new method, and photolysis processes through channels (1) and (2) are simulated in the third section by using molecular dynamics. Simulation results are examined in the final section.

Trapping-Site Structures

We have developed a statistical ensemble model to describe the codeposition of guest and host molecules (host/guest ~ 1000) from the gas phase onto a cold surface. Based on this model, a novel molecular dynamics method is proposed to simulate the trapping-site structures.[6] The reliability of this method has been confirmed not only by the vibrational frequency shift of BrO, ClO, CN, CS, NCl, NBr in argon matrices with respect to that in the gas phase, but also by the relative probabilities for the formation of single-, double-, and multiple-substitutional trapping sites of NBr.

The procedure for determining the trapping-site structure of O_3 in an argon matrix is the same as that described in detail previously.[6] Briefly, we construct an argon matrix, M, containing $5 \times 5 \times 5$ fcc unit cells in a cubic arrangement (the lattice constant $a = 0.532$ nm) with an O_3 molecule substituting one argon atom of the innermost unit cell. The boundary atoms, except for the top ones of M, are fixed in position to construct the walls of a cold reservoir, and the other atoms of M (including the top ones) as well as the oxygen atoms in the ozone molecule are mobile in classical trajectories. A fourth order Runge–Kutta method is used to compute the trajectories with a fixed step size of 3 fs. The geometry of M is allowed to relax for about 300 fs at the deposition temperature, T_D (10 K). We then let the time of the system go backwards by integrating Hamiltonian motion equations with a negative time step and using the velocity reset method in an inverse manner, which means the past velocities of the boundary atoms are obtained by superposing the velocities of the Maxwell distribution upon their present velocities.[6,7] As the time goes backwards, the system goes back to its past (to the gas phase) with the average kinetic energy of the atoms increasing. When the kinetic energy is greater than that needed to escape the valley of the potential for argon atoms (120 K), we let the system relax adiabatically for a long period of time. During that period, we take samples every 1 ps from the states of the system as initial conditions to simulate the deposition process by cooling the system with the velocity reset method.[7] When the temperature of the system is close to 10 K, a damped trajectory method[8] is used to search for the equilibrium structure, and then the normal mode of O_3 is calculated.

In our calculations, the interaction potential for argon atoms is taken as a Lennard–Jones function, as is the potential for the argon atom and the oxygen atom in O_3. The potential parameters are the same as those presented in ref. 9. The potential surface of O_3 is taken from ref. 10. For calculating normal modes, the total potential of O_3 is written as the sum of Lennard–Jones potentials for Ar + O and the molecular potential of ozone.

The deposition procedures were performed a total of 40 times. It is shown that the most frequently formed sites (35 of 40) are singly substituted (SS) ones. In this SS cage, O_3 replaces an argon atom and the direction of the larger dimension of the molecule vibrates about the C_4 axis of the site (Fig. 1). The calculated normal frequency (ν_3) shifts with respect to that of free ozone are either red by 6 cm^{-1} (23 of 35) or blue by 7 cm^{-1} (9 of 35) in the SS sites. The probability for double substitution (DS) sites is quite low (1 of 40). The calculated frequency (ν_3) shift in the DS site is blue by 55 cm^{-1}.

Benderskii and Wight observed that the frequency (ν_3) shifts of O_3 isolated in an argon matrix are red by 0.5 cm^{-1} and blue by 1.2 cm^{-1},[2] which are nearer to the frequency (ν_3) shifts calculated in the SS site than in the DS site. The discrep-

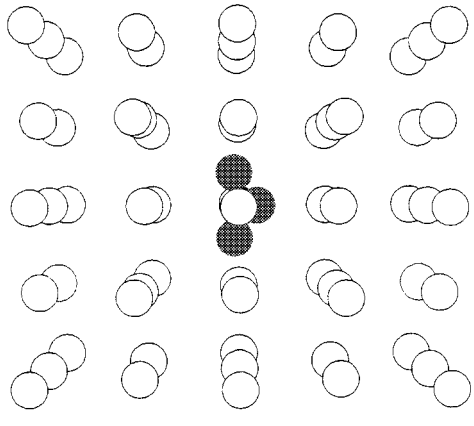

FIGURE 1. A single substitutional site of O_3 isolated in an argon matrix.

ancy between our calculated shifts and the experimental measurements is caused mainly by neglecting the anharmonic terms in the normal mode consideration used.

Simulation of O_3 Photolysis in Matrices

Hartley band ultraviolet (UV) absorption of O_3 involves four electronic states, which are depicted in Figure 2. UV photolysis of free ozone molecule has been extensively investigated both theoretically and experimentally.[11,12] The conclusion is that photoexcitation populates the $^1B_2$ state, which either dissociates into $O_2(^1\Delta_g)$ + $O(^1D)$ with a quantum yield of 0.9 (channel (1)) or crosses with a repulsive state, R, producing fragments of $O_2(^3\Sigma_g^-)$ + $O(^3P)$ with a quantum yield of 0.1 (channel (2)). The 2^1A_1 state is expected to play a lesser role in the photochemistry, because it corresponds to two-electron excitation.[12]

The UV photolysis of ozone isolated in a matrix should be different from that of free ozone because of matrix cage effects. We carried out a molecular dynamics simulation on the photodissociation of O_3 in an argon matrix with 266-nm irradiation. This corresponds to a photon energy of 4.66 eV, which is the minimum value needed to excite the molecular transition from the minimum of the X^1A_1 surface to the $^1B_2$ state vertically.

The model for the simulation is similar to that used by Raff et al.,[13,14] except that the trapping-site structure of O_3 in solid argon is determined by our new method (see previous section). It should be stressed that the transport effects of the bulk are simulated using the velocity reset method with the parameters presented in ref. 14. At the beginning, the ozone molecule in ground state X^1A_1 is allowed to relax in an Ar matrix at the temperature of 10 K (or 20 K). At random timepoints, the potential surface corresponding to the $^1B_2$ state is switched on (photon excitation), without changing the positions and momentum of the atoms in the O_3 molecule (Frank–Condon principle). The classical trajectories are calculated by a fourth order Runge–Kutta method with a fixed step size of 0.25 fs. It has been noted that most of the photodissociation of the guest molecules in cryogenic matrices takes place within the first picosecond[15–18] so the trajectory of the system is computed for a duration of 1 ps. The fraction of runs that leads to the separation of the O atom from O_2 by more than one lattice distance (0.532 nm) gives the photodissociation quantum yield ϕ.[17]

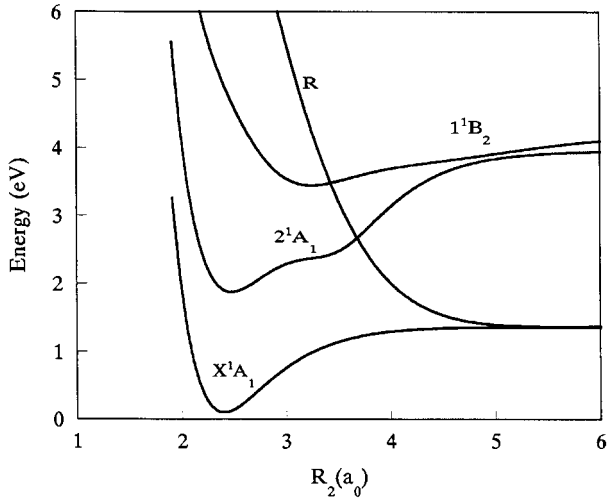

FIGURE 2. Potential energy curves for $O_3 \rightarrow O_2 + O$ by varying one bond length (R_2) and fixing the other geometrical parameters at $\theta_1 = 110°$ and $R_1 = 2.5\ a_0$.

The potential surfaces of $^1B_2$, X^1A_1, and 2^1A_1 are taken from refs. 12, 10, and 19, respectively. The potential surface of R is obtained by fitting the data presented in ref. 11 with an approximate function:

$$\begin{aligned} V_R = 6.456\Big\{ & A_1[1 - \exp(-1.118(R_2 - 1.2075))]^2 \\ & + A_2[1 - \exp(-1.118(R_1 - 1.2075))]^2\Big\} \\ & + 120\sum_i^3 A_i \exp[-1.5(R_i - 1.2075)]^2 \\ & + 0.035\exp\Big\{-0.51\Big[(R_1 - 1.2075)^2 \\ & + (R_2 - 1.2075)^2\Big]\Big\} \times \Big[(\theta_1 - 2.038)^2 \\ & + (\theta_2 - 0.551)^2 + (\theta_3 - 0.551)^2\Big] \qquad \text{(eV)} \end{aligned}$$

with:

$$A_i = |\tanh(0.3(R_i - 1.2075))| \qquad i = 1, 2, 3$$

where θ_i and R_i $(i = 1, 2, 3)$ are as depicted in Figure 3.

The Lennard–Jones pairwise potentials for argon atoms are the same as those described in the previous section. The parameters of the Lennard–Jones potential for O interacting with Ar are determined according to the atomic states related to the electronic states of O_3.[20] When O_3 is in the X^1A_1 or R state, the potential parameters for O and Ar are obtained by fitting the potential energy curve $^3\Sigma^-$ for $Ar(^1S) + O(^3P)$, because both the X^1A_1 and the

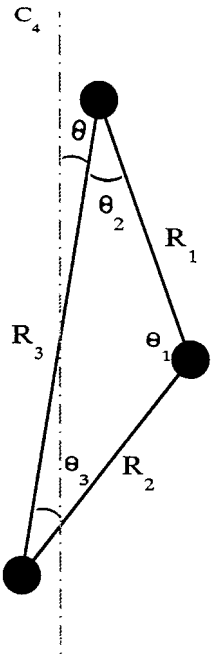

FIGURE 3. Parameters θ, θ_i and R_i used for R potential surface of O_3.

R states dissociate to $O(^3P)$ and O_2 $(^3\Sigma_g^-)$, which arises from the combination of two separated $O(^3P)$ atoms. The potential parameters determined in this way are very close to those used in ref. 9. The $^1B_2$ state correlates with $O_2(^1\Delta_g) + O(^1D)$, and thus the parameters of the Lennard–Jones function are determined by fitting the potential energy curve for Ar $(^1S) + O(^1D)$. There are three different potential curves $(^1\Sigma^+, ^1\Pi$, and $^1\Delta)$ for Ar $(^1S) + O(^1D)$.[20] We consider that the potential curve in an argon matrix should be an average over these three curves because of the perturbation of the lattice atoms. An average potential curve is obtained in the following way: for a given potential energy, the distance between Ar and O is determined by averaging over the three distances correlated to the curves $^1\Sigma^+$, $^1\Pi$, and $^1\Delta$, respectively.[20]

Six hundred trajectories on the $^1B_2$ surface (channel (1)) were calculated for O_3 trapped in argon matrices at 10 K and 20 K, respectively. The quantum yields of photodissociation were found to be 0.01 ± 0.002 for both 10 K and 20 K temperatures, which are about one order of magnitude smaller than that of free O_3. It is evident that the photodissociation of O_3 through channel (1) is hindered efficiently by the matrix cage. It is clear that the matrix temperature does not influence the quantum yield of channel (1).

Eight hundred trajectories were calculated with channel (2). Initially, O_3 is in the $^1B_2$ state, and then ''jumps'' into the R state after the crossing of the two potential surfaces, and finally lies in the X^1A_1 state when the distance of the O atom from O_2 was larger than 0.5 nm. In 400 trajectories, the photolysis quantum yield for Ar matrix at 20 K was found to be 0.03 ± 0.005. When the matrix was at 10 K, no photolysis of O_3 through channel (2) was observed in 400 trajectories.

The temperature effect on the quantum yield can be understood by examining the vibration of ground state O_3 in the matrix. The angle subtended between an internuclear axis of O_3 (cf. Fig. 3) and the C_4 axis was designated by θ. The time evolution of θ is shown in Figure 4 for 20 ps. For the matrix at 20 K, θ oscillated between 0° and 25° (dashed line in Fig. 4). The oscillation amplitude of θ decreased to 15° when the matrix was at 10 K (solid line in Fig. 4). Taking the crystalline structure (fcc) of the Ar matrix into account, the Ar atoms located along the C_4 symmetric axes hindered the departure of O from O_2. It has been noted that the photodissociation of some diatomic molecules in rare-gas matrices takes place only if θ is large enough.[16,17] Thus, photolysis of O_3 in the argon matrix at 20 K should be more probable than that of O_3 in the argon matrix at 10 K.

The simulations just examined began with O_3 located in a single substitution site, which is the most probable site determined in previous section. If we construct a double substitutional site for an O_3, the corresponding simulations show that the photolysis quantum yield is near unity at both 10 K and 20 K temperatures. Obviously, the dynami-

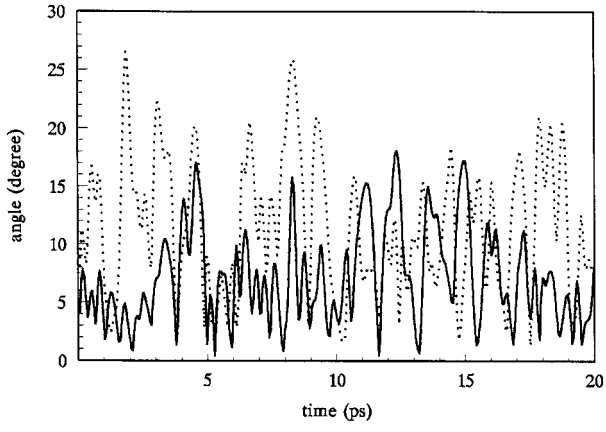

FIGURE 4. Variation in time of O_3 orientation in a single substitutional trapping site of an argon matrix at 10 K (solid line) and 20 K (dashed line).

cal process is largely dependent on the trapping-site structures.

Discussion

Benderskii and Wight experimentally studied the photochemistry of ozone trapped in argon matrices at 10–30 K using 266-nm laser irradiation.[2] They carefully measured the quantum yield of O_3 photolysis and found it to be sensitive to matrix temperature. Based on our theoretical simulations, the experimental results can be used to establish a picture of O_3 photolysis in argon matrices.

As pointed by other investigators,[11,12] channel (1) is more important than channel (2) for the UV photodissociation of free O_3, because the quantum yield through channel (1) is close to unity. When O_3 is isolated in an Ar matrix, our simulations in the previous section showed that the quantum yield through channel (1) decreased to 0.01 for the matrix at both 10 K and 20 K. If channel (1) was still the principal channel for UV photodissociation of O_3 in the matrix, then we cannot explain the experimental result that the quantum yield for the matrix at 20 K was ninefold larger than that of the matrix at 10 K.[2] Therefore, channel (2) should play a more important role in this case.

In fact, there are three possible channels for the O_3 in the $^1B_2$ state to lose its energy. In addition to channels (1) and (2), the spontaneous transition from the $^1B_2$ state to the other state represents a third channel. In general, the lifetime of a bound electronic state is about several tens of nanoseconds, and therefore the spontaneous transition can be ignored in the reaction dynamics. On the other hand, the transfer efficiency of O_3 from $^1B_2$ to R should be very high when O_3 is trapped in the matrix. Based on the fact that the quantum yield of free O_3 via channel (2) is about 0.1,[11,12] we can suggest that about 10% of the population of $^1B_2$ transfers to R after the crossing of $^1B_2$ and R surfaces. In matrices, the dissociation of O_3 on the $^1B_2$ surface is hindered by the matrix cage, so there are many opportunities for O_3 along the $^1B_2$ surface going through the cross region of $^1B_2$ and R, which causes most of the population to transfer from $^1B_2$ to R. Consequently, channel (2) should be the principal channel for the O_3 in matrices to lose its energy.

According to our simulation results of UV photodissociation of O_3 in the SS trapping site of Ar matrices, the quantum yields through channel (2) increase with the matrix temperature, and the total quantum yields (including both photolysis channels) are 0.01 and 0.04 for the matrix at 10 K and 20 K, respectively. Within experimental error,[2] our theoretical quantum yields are in agreement with the experimental measurements: 0.007 ± 0.004 and 0.06 ± 0.03 for the matrix at 10 K and 20 K, respectively. Obviously, channel (2) is more important in the UV photodissociation of O_3 in Ar matrices.

It is clear that the most probable trapping site of O_3 in Ar matrices should be SS, because the quantum yields calculated with the DS trapping site are close to unity, which is much higher than experimental measurement. Furthermore, our simulations in the second section show that the most probable trapping site is SS and the probability of DS site formation is very low.

Conclusions

The most probable trapping site of O_3 isolated in an argon matrix was found to be single substitutional by a technique of time reversal. The calculated matrix shifts (v_3) of O_3 in this trapping site were close to the experimental measurements. In addition, we conducted MD dynamics simulations of the UV photodissociation of O_3 in Ar matrices. It has been shown that the photolysis channels of O_3 in the SS trapping site are seriously hindered by the matrix cage and channel (2) is more important in UV photodissociation of O_3 in Ar matrices. The photolysis quantum yield via channel (2) was shown to be sensitive to matrix temperatures.

References

1. Steinfeld, J. I.; Adler-Golden, S. M.; Gallagher, J. W. J Chem Phys Ref Data 1987, 16, 911 (and references therein).
2. Benderskii, A. V.; Wight, C. A. J Chem Phys 1994, 101, 292.
3. Benderskii, A. V.; Wight, C. A. Chem Phys 1994, 189, 307.
4. Leforestier, C.; LeQuere, F.; Yamashita, K.; Morokuma, K. J Chem Phys 1994, 101, 3806.
5. Okabe, H. Photochemistry of Small Molecules; Wiley-Interscience: New York; 1978.
6. Ning, X.-J.; Qin, Q. Z. J Chem Phys. In press.
7. Riley, M. E.; Coltrin, M. E. J Chem Phys 1988, 88, 5934.
8. Raff, L. M. J Chem Phys 1990, 93, 3160.
9. Samuni, U.; Fraenkel, R.; Haas, Y.; Fajgar, R.; Pola, J. J Am Chem Soc 1996, 118, 3687.

10. Varandas, A. J. C.; Murrell, J. N. Chem Phys Lett 1982, 88, 1.
11. Hay, P. J.; Pack, R. T.; Walker, R. B.; Heller, E. J. J Phys Chem 1982, 86, 862 (and references therein).
12. Sherppard, M. G.; Walker, R. B. J Chem Phys 1983, 78, 7191 (and references therein).
13. Raff, L. M. J Chem Phys 1990, 93, 3160 and 1991, 95, 8901.
14. Ford, M. B.; Foxworthy, A. D.; Mains, G. J.; Raff, L. M. J Phys Chem 1993, 97, 12134.
15. Alimi, R.; Gerber, R. B.; Apkarian, V. A. J Chem Phys 1988, 89, 174.
16. Alimi, R.; Brokman, A.; Gerber, R. B. J Chem Phys 1989, 91, 1611.
17. Alimi, R.; Gerber, R. B.; Apkarian, V. A. J Chem Phys 1990, 92, 3551.
18. Agrawal, P. M.; Sorescu, D. C.; Raff, L. M. J Phys Chem 1995, 99, 14959.
19. Carter, S.; Mills, I. M.; Murrell, J. N.; Varandas, A. J. C. Mol Phys 1982, 45, 1053.
20. Dunning, T. H., Jr; Jeffery Hay, P. J. Chem Phys 1977, 66, 3767.